A numerical investigation on the ignition of JP-8 surrogates blended with hydrogen and syngas

Suresh Aggarwal, Thomas Helma & Dongru Li

International Journal of Advances in Engineering Sciences and Applied Mathematics

ISSN 0975-0770
Volume 6
Combined 1-2

Int J Adv Eng Sci Appl Math (2014)
6:49-64
DOI 10.1007/s12572-014-0111-0

Springer

Your article is protected by copyright and all rights are held exclusively by Indian Institute of Technology Madras. This e-offprint is for personal use only and shall not be self-archived in electronic repositories. If you wish to self-archive your article, please use the accepted manuscript version for posting on your own website. You may further deposit the accepted manuscript version in any repository, provided it is only made publicly available 12 months after official publication or later and provided acknowledgement is given to the original source of publication and a link is inserted to the published article on Springer's website. The link must be accompanied by the following text: "The final publication is available at link.springer.com".

Author's personal copy

Int J Adv Eng Sci Appl Math (January–June 2014) 6(1–2):49–64
DOI 10.1007/s12572-014-0111-0

IIT, Madras

A numerical investigation on the ignition of JP-8 surrogates blended with hydrogen and syngas

Suresh Aggarwal · Thomas Helma · Dongru Li

Published online: 19 June 2014
© Indian Institute of Technology Madras 2014

Abstract A numerical study is conducted to characterize the hydrogen- and syngas-assisted ignition of two JP-8 surrogates, a two-component surrogate and a six-component surrogate. The six-component surrogate has previously been found to accurately simulate the smoke point, volatility, flame temperature profiles, and extinction limits of JP-8, while the two component surrogates has been shown to reproduce the flame structure predicted with the six-component surrogate. CHEMKIN 10101 software along with the CRECK-0810 kinetic mechanism, involving 341 species and 9,173 reactions, is used to simulate ignition in a closed homogenous reactor under adiabatic and isobaric conditions. While the mechanism has been previously validated against various targets involving JP-8 surrogates, additional validation is provided herein for the ignition of H_2, syngas, and *n*-dodecane. Results focus on the effects of H_2 and syngas on the ignition of JP-8 surrogates at engine relevant conditions. For $650 < T < 1{,}000$ K, the ignition of JP-8 surrogates exhibits the classical two-stage ignition and negative temperature coefficient (NTC) behavior, characterized by two competing paths. The first path is favored at low temperatures ($T < 800$ K) and involves ketohydroperoxide radicals, which decompose and increase the system reactivity. The second path becomes dominant in the NTC region ($800 < T < 1{,}000$ K), and involves the decomposition of alkyl and alkylhydroperoxy radicals with a drop in system reactivity. The addition of H_2 or syngas in relatively small quantity has no effect on the ignition of surrogates, whereas H_2 or syngas in larger amounts (more than 80 % by volume) increases and decreases the ignition delays of surrogates at low and high temperatures, respectively. The increase in ignition delay due to H_2 addition can be attributed to reaction: $H_2 + OH = H_2O + H$, which depletes OH radicals and slows down the ignition process. On the other hand, for $T > 1{,}000$ K, the addition of H_2 reduces ignition delay due to reactions: $H_2O_2 + M = 2OH + M$, $H_2 + OH = H_2O + H$, $H + O_2 = OH + O$, and $H + HO_2 = OH + OH$, which produce ample OH radicals, and accelerate the ignition process. The presence of CO reduces the effectiveness of reaction: $H_2 + OH = H_2O + H$, and thus decreases the ignition delays of JP8/syngas blends in the low temperature and NTC regions. For the conditions investigated, the ignition characteristics of JP-8 surrogates, including the two-stage ignition and NTC behavior, can be well represented qualitatively by *n*-dodecane. Although the two surrogates studied here represent the JP-8 fuel, results are also relevant for other liquid fuels, such as gasoline and diesel fuels, which generally contain straight-chain (*n*- and *iso*-), branched-chain, and cyclo-paraffins, and aromatics.

Keywords Ignition · JP-8 surrogate/H_2 blends · JP-8 surrogate/syngas blends · Reaction pathways

S. Aggarwal (✉) · T. Helma · D. Li
Department of Mechanical and Industrial Engineering, University of Illinois at Chicago, 842 W. Taylor St, Chicago, IL 60607, USA
e-mail: ska@uic.edu

1 Introduction

Biomass-derived fuels, especially from non-food and locally available sources, have the potential to meet a significant part of the global energy need in an environmentally friendly manner. Hydrogen (H_2) and syngas (blend of H_2 and CO) are two such renewable fuels, which can be produced from a number of biomass sources using a variety of biological, thermochemical, and physical processes [1–4]. In addition, these fuels have many desirable

Author's personal copy

combustion characteristics, including high energy content per unit mass, wide flammability limits, high burning velocities, and low emissions. There are also many challenges associated with the use of these fuels, such as storage and volumetric energy content of H_2, and wide variation in syngas composition. In order to address these challenges, a blended fuel approach, based on using an appropriate mixture of petroleum-based fuels and syngas (or H_2) seems quite promising. Such an approach can exploit the advantages associated with each fuel, while mitigating their disadvantages. It also has the potential of increasing the use of renewable fuels within the existing infrastructure, and providing greater flexibility in the design and operability of combustion systems.

Numerous studies have examined the viability of blended fuel strategy in reducing emissions of greenhouse gas and other pollutants, while maintaining or improving efficiencies of the existing combustion devices. Examples include various bio/petroleum [5], natural gas/gasoline [6], and H_2/natural gas blends [7], which are being used or tested in different transport and power generation systems. Extensive research has also been reported concerning the effect of H_2 on the combustion and emission behavior of petroleum-based fuels in various flame and engine configurations [8]. A number of fundamental studies have investigated the effect of H_2 addition on the flammability limits [9], burning velocities [10–12], flame stability [13], lame speed-stretch interactions and Markstein lengths [11, 14], NO_x emissions [9, 15–17], and lean blowout limits [18, 19] of methane flames. Different flame configurations, including laminar premixed [10, 11, 20], nonpremixed [17] and partially premixed flames [14, 15], as well as burner stabilized [21, 22] and swirl-stabilized [18, 23] turbulent flames have been employed. The ignition characteristics of H_2-enriched methane-air mixtures have also been investigated using rapid compression machine (RCM) [24] and [25] shock tube facilities. Fotache et al. [26] investigated the effect of H_2 on methane ignition in a counterflow diffusion flame, and identified three ignition regimes, namely, hydrogen-assisted, transition, and hydrogen-dominated, based on the H_2 fraction in the blend.

There have also been studies examining the use of H_2 in engines operating in a dual fuel mode. Various hydrocarbon (HC)–H_2 blends, such as CH_4–H_2 [27–29], natural gas (NG)–H_2 [30–35], and gasoline–H_2 [36, 37] blends have been considered, and the effect of H_2 on engine performance and emission has been examined. Some limited work has also been reported on the use of H_2 [38] and syngas [39] in dual fuel diesel engines. A general observation from these studies is that the use of H_2 generally leads to an improvement in fuel efficiency and performance, although the actual effect depends on the operating conditions and various other factors, such as compression ratio, equivalence ratio, spark timing, engine speed and load, etc. For instance, due to the low ignition energy and high burning velocity associated with H_2, the use of a HC–H_2 blend in SI engines accelerates flame initiation and propagation, which reduces combustion duration and leads to improved combustion efficiency, especially when the spark timing is optimized. In general, the addition of moderate amounts of H_2 to HC-fueled SI engines can decrease BSFC (brake specific fuel consumption), especially at lean burning conditions and higher engine speeds. The HC, CO, and CO_2 emissions also decrease with H_2 addition due to the replacement of HC fuel by H_2. While the NO_x emission increases with H_2 addition at a fixed equivalence ratio, the use of H_2 enables operation with leaner mixtures without increasing combustion duration, which reduces NO_x emissions without sacrificing engine output and efficiency. Moreover, the amount of EGR can be increased with H_2 addition, which further reduces NO_x. Similarly, the addition of H_2 to HCCI engines can significantly enhance the ignition reliability, provide more homogeneous ignition, and expand the operation range of equivalence ratios and engine loads [40].

The literature review indicates that compared to CH_4/H_2 blends, there have been few studies dealing with blends of H_2 with heavier (or liquid) fuels. Subramanian et al. [41] examined the effect of H_2 and CO on the autoignition of homogeneous *n*-heptane/air mixtures, while Thiessen et al. [42] investigated the ignition of *n*-C_7H_{16}/H_2 and *n*-C_7H_{16}/CH_4 blends. Aggarwal et al. [43] reported a numerical study on the effect of H_2 and CH_4 addition on the ignition of *n*-heptane/air mixtures at engine relevant condition. Results indicated that for H_2 or CH_4 mole fractions less than 80 % in the blend, the ignition is predominantly determined by the *n*-C_7H_{16} oxidation chemistry. As these mole fractions are increased above 80 %, the presence of H_2 was found to increase and decrease ignition delay at low ($T < 900$ K) and high ($T > 1{,}000$ K) temperatures, respectively, while that of CH_4 increased ignition delay at all temperatures. Furthermore, the sensitivity analysis indicated that the heptyl and hydroxyl radicals play the key role in determining the ignition behavior of *n*-C_7H_{16}/H_2 and *n*-C_7H_{16}/CH_4 blends. Jain et al. [44] subsequently examined the effect of H_2 and syngas on the ignition of *iso*-C_8H_{18}/air mixtures at engine relevant conditions. The ignition behavior of *iso*-C_8H_{18}/H_2 blends was found to be generally similar to that of *n*-C_7H_{16}/H_2 blends. Thus, for H_2 mole fractions above 80 %, the presence of H_2 increases the ignition delay at low temperature, and increases it high temperature. Furthermore, the rate of production analysis indicated that at low temperatures, H_2 addition in significant amount (more than 80 % by volume) consumes hydroxyl radicals via $H_2 + OH = H_2O + H$, and slows down *iso*-C_8H_{18} ignition chemistry, and increases ignition delay. In contrast, at high temperatures, the decrease in ignition delay due to H_2 addition can be attributed to chain branching reactions $O_2 + H = OH + O$ and $H_2O_2 + M = OH + OH + M$.

Author's personal copy

The literature review further indicates that previous studies dealing with H_2 or syngas-assisted ignition/combustion of hydrocarbon fuels have only considered pure fuels, while most practical fuels are a mixture of a large number of chemical species. A particularly challenging aspect of modeling such fuels is their highly complex chemical structure containing hundreds of molecular species, including straight-chain, branched-chain, and cyclo-paraffins, as well as aromatics and additives. Consequently, developing reliable kinetic and thermo-transport models to simulate their combustion and emission characteristics even in simple configurations is prohibitively challenging. A more commonly followed approach is to formulate appropriate surrogate mixtures that can emulate the physical and chemical characteristics of real fuels over a broad range of conditions. These surrogates are usually defined either as a physical surrogate, a mixture that mimics the physical properties of the fuel, or a chemical surrogate, a mixture that mimics the chemical-class composition and molecular weight of the fuel [45]. A common strategy is to use a surrogate blend of a relatively small number of pure hydrocarbons, and control the molar fractions of constituent components in order to reproduce the combustion behavior of the actual fuel with respect to certain targets. Such targets include hydrogen to carbon ratio, critical conditions of autoignition and extinction, laminar flame speed, and emission characteristics. At the next level of validation, targets may include flame liftoff height, species profiles during pyrolysis/oxidation, flame structure, etc.

Based on the above strategy, a number of surrogates have been explored [46, 47], and detailed chemistry and transport models have been developed. Far et al. [48] studied the flame structure and laminar burning speed of JP-8/air mixtures at high temperatures and pressures. Several researchers have employed a counterflow burner [49, 50] and investigated premixed [13, 51], and non-premixed flames [14, 52] using various JP-8 surrogates. Other studies have examined the sooting characteristics [53, 54], NO_x [55], flame stability [16], and flammability limits [56]. The ignition of JP-8 and its surrogates have also been examined. Vasu et al. [57] reported JP-8 shock tube ignition data for temperatures between 715 and 1,229 K, pressures 17–51 atm, and equivalence ratios of 0.5 and 1.0. Kumar and Sung [58] reported RCM data for the ignition of JP-8 for temperatures between 650 and 1,100 K, pressures of 7, 15, and 30 bar, and equivalence ratios between 0.42 and 2.26. While there have been numerous studies on the combustion of JP-8 and its proposed surrogates, the effect of H_2 and syngas addition on the ignition and combustion characteristics of JP-8 and surrogates have not been investigated.

The present study aims to extend the previous work dealing with H_2 or syngas-assisted ignition of pure hydrocarbons to real fuels containing a mixture of components. Based on the literature review, two representative surrogates, namely, a two-component surrogate [59] and a six-component surrogate [60], were selected for the present investigation. As reported by Katta and Roquemore [61], these two surrogates have nearly identical flame structures, suggesting that they were formulated to represent the same JP-8 fuel. Moreover, the six-component surrogate has been shown to accurately simulate the smoke point and volatility [60], as well as flame temperature profiles and extinction limits [50] of JP-8. It is also important to note while these surrogates represent the JP-8 fuel, the present study is also applicable to other liquid fuels, including gasoline and diesel fuels, which typically contain straight-chain (*n*- and *iso*-), branched-chain, and cyclo-paraffins, and aromatics.

Our focus is on ignition under homogeneous, quiescent conditions so as to isolate chemical kinetic effects from fluid dynamics effects. Simulations were performed to characterize the effects of H_2 and syngas addition on the ignition of surrogates and their individual components. For the conditions investigated, results indicated that the ignition behavior of these two surrogates is predominantly determined by the *n*-dodecane (n-$C_{12}H_{26}$) ignition chemistry. Consequently, the dominant reactions influencing the ignition of these blends were identified through a detailed sensitivity analysis using n-$C_{12}H_{26}$/H_2/CO mixtures. The analysis also highlighted the main paths for the ignition of these blends, and provided insight into the effects of H_2 and syngas on the ignition of surrogates at engine relevant conditions. The remainder of the paper is organized as follows. The numerical model and the two surrogates used in the present study are briefly described in Sect. 2. Results on the effects of H_2 and syngas on the ignition of the two surrogates and their components, as well as the sensitivity and reaction path analysis, are presented in Sect. 3. Concluding remarks are provided in the final section.

2 Numerical model

The two JP-8 surrogates used in the present study are listed in Table 1. The first surrogate (SERDP) has two components, namely, *n*-dodecane and *m*-xylene, while the second one (Violi surrogate) is composed of *n*-dodecane, *n*-tetradecane, *iso*-octane, methylcyclohexane (MCH), *m*-xylene, and tetralin. The CHEMKIN 10101 software was used to simulate ignition under constant pressure and adiabatic conditions. The software uses implicit time integration schemes as described in Ref. [62] to solve the transient, spatially homogeneous forms of the mass and energy conservation equations. The state of ignition was defined as the point where the rate of change of temperature exceeded a predefined value. Using a different

Author's personal copy

Table 1 JP-8 surrogate fuels

Surrogate compound	Molecular formula	Violi surrogate	SERDP surrogate
n-Dodecane	n-$C_{12}H_{26}$	30	77
n-Tetradecane	n-$C_{14}H_{30}$	20	
iso-Octane	C_8H_{18}	10	
Methylcyclohexane	C_7H_{14}	20	
m-Xylene	C_8H_{10}	15	23
Tetralin	$C_{10}H_{12}$	5	

criterion based on the temporal evolution of hydroxyl radical yielded identical results.

Simulations were performed using the CRECK-0810 mechanism [63], which is a detailed kinetic model involving 341 species and 9,173 reactions, and has been extensively validated against flame measurements with a number of hydrocarbon fuels. It has also been shown to reproduce the low temperature oxidation behavior of several pure and multi-component fuels [64], as well as the measured NTC (negative temperature coefficient) ignition behavior of JP-8 [57]. Since the present study considers blends of H_2/syngas with JP-8 surrogates with *n*-dodecane being a major constituent, the mechanism was further validated for predicting the ignition delays for H_2, syngas, and *n*-dodecane fuels at relevant conditions. As indicated in Fig. 1a, there is excellent agreement between the ignition delays for H_2-air mixtures predicted using the CRECK-0810 mechanism and the Conaire mechanism [65], which has been extensively validated for H_2 oxidation against a variety of targets. Figure 1b presents a comparison of predicted ignition delays using the CRECK-0810 mechanism and the revised Davis et al. [66] mechanism with the shock tube measurements of Petersen et al. [67] for syngas-air mixtures at $P = 20$ atm and $\phi = 0.5$. Predictions show good agreement with measurements for $T > 1{,}000$ K. However, there are significant differences below 1,000 K. As discussed in previous studies [67, 68], such differences at low temperatures can be attributed to mixture non-homogeneities, which are present in RCM experiments but cannot be reproduced in simulations. The CRECK-0810 mechanism was found to predict somewhat shorter ignition delays compared to the Davis mechanism, but provide closer agreement with measurements. Finally, a comparison of predictions and shock tube measurements of Vasu et al. [57] for the ignition of *n*-dodecane/air mixtures is presented in Fig. 1c. There is fairly good agreement between predictions and measurements, especially for temperatures above 930 K. For temperatures below 930 K, there are some discrepancies, which are generally within the measurement uncertainty. More importantly, the mechanism reproduces the experimentally observed NTC region.

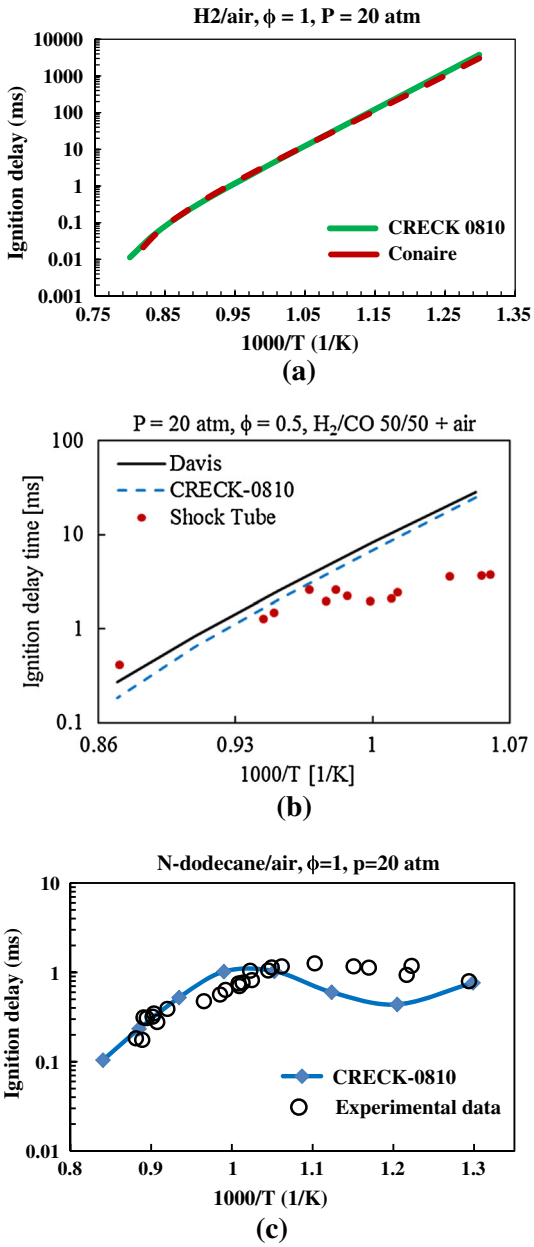

Fig. 1 Comparison of ignition delay predictions using the CRECK-0810 mechanism with (*a*) predictions of Conaire mechanism for H_2-air mixtures at $P = 20$ atm and $\phi = 1.0$, (*b*) predictions of Davis mechanism and shock tube measurements of Petersen et al. [66] for syngas-air mixtures at $P = 20$ atm, and $\phi = 0.5$, and (*c*) shock tube measurements (*open circle*) of Vasu et al. [57] for *n*-dodecane/air mixtures at $P = 20$ atm and $\phi = 1.0$. The shock tube measured data in (*c*) is normalized to a pressure of 20 atm

3 Results and discussion

Results first consider the effects of H_2 or syngas on the ignition of individual components of each surrogate, and then on the ignition of surrogates. The component that is most responsible for the observed ignition behavior of surrogates is also identified. Finally, the results of

Author's personal copy

sensitivity and reaction path analysis are presented to provide further insight into the effects of H_2 and syngas on the ignition of JP-8 surrogates. Important pathways and reactions responsible for the observed ignition behavior of blends are also identified.

3.1 Ignition of component/H_2-air mixtures

Figure 2 presents results concerning the effect of H_2 on the ignition of individual components of the two JP-8 surrogates. For each case, the ignition delay time is plotted as a function of temperature for different blend compositions with 0, 10, and 90 % H_2 by volume. For four of the six components (i.e., *n*-dodecane, *n*-tetradecane, *iso*-octane, and MCH), the ignition delay (t_{ig}) exhibits the expected NTC (negative temperature coefficient) behavior for temperatures between 800 and 1,000 K, where the ignition delay decreases as the temperature is reduced.[1] For temperatures outside the NTC region, the ignition delay increases with the decrease in temperature.[2] For the two aromatic components (i.e., *m*-xylene and tetralin), the NTC region is not observed. As discussed in the literature [49], the NTC behavior is associated with the oxidation chemistry of large straight-chain and branch-chain alkanes and alkenes. However, the effect of H_2 addition seems to be qualitatively the same for all six components. H_2 addition in small amounts has essentially no effect on the ignition behavior of the components, implying that the chemistry is dominated by the hydrocarbon fuel oxidation. On the other hand, H_2 addition in larger amount (more than 80 % by volume) increases and decreases the ignition delays at low ($T < 1{,}000$ K) and high ($T > 1{,}000$ K) temperatures, respectively. For the two alkane components (*n*-dodacane and tetradecane), it is also interesting to note that even with 90 % H_2, the ignition delay exhibits the NTC behavior, implying that the alkane chemistry still plays a significant role. These results are consistent with those reported previously by Subramanian et al. [41] and Aggarwal et al. [43] for the ignition of *n*-C_7H_{16}/H_2 blends.

3.2 Effect of components on the ignition of surrogate

Simulations were performed to determine as to which surrogate component plays a more significant role in determining the observed ignition behavior of the surrogate. Figure 3 plots ignition delay time as a function of temperature for the SERDP surrogate and its two components, without H_2 or syngas addition. Ignition delay plots for the entire temperature range including the NTC region are essentially the same for the surrogate and *n*-dodecane, implying that the ignition behavior of this surrogate can effectively be represented by *n*-dodecane. Figure 4 presents the ignition delay plots for the Violi surrogate and each of its six components. There are several important observations from this figure. One, the ignition of surrogate including its NTC behavior is qualitatively similar to that of four of its components; namely *n*-dodecane, *n*-tetradecane, *iso*-octane, and methylcyclohexane. Note that the NTC behavior is that obvious for *iso*-octane due to the temperature range used in Fig. 4. However the existence of NTC region *iso*-octane has been demonstrated in other studies [44]. Two, the ignition delay times are the shortest for *n*-dodecane and the longest for tetralin. Three, the ignition behavior of surrogate can be reasonably well simulated by its two *n*-alkane components, namely *n*-dodecane and *n*-tetradecane. The effect of other components is to increase the ignition delay time of the surrogate and moderate its NTC dropoff. Thus, an important observation from Figs. 3 and 4 is that the ignition behavior of the surrogates can be reasonably well represented by *n*-dodecane, although there are some quantitative differences. In Sect. 3.4, this result is further confirmed through the temporal evolution of key radical species during the ignition process.

3.3 Ignition of JP-8 surrogate/H_2/CO blends

Figure 5 presents the predicted ignition delays for different SERDP/H_2/CO blends, with the first three blends containing 0, 10, and 90 % H_2 by volume, and the other two containing 10 and 90 % syngas (50 % H_2/50 % CO) by volume. For all five cases, the ignition delays exhibit NTC behavior. Furthermore, results indicate that H_2 or syngas addition in small quantities has no effect on the ignition of SERDP blend. However, their addition in larger amounts increases the ignition delay time at low temperatures including the NTC region, and decreases it at high temperatures ($T > 1{,}000$ K). Results for the Violi surrogate/H_2/CO blends, presented in Fig. 6, exhibit similar behavior as that for the SERDP/H_2/CO blends. Again, H_2 or syngas addition in relatively small quantity has no effect on the ignition delays. However, their addition in large quantities (more than 80 % by volume) increases the ignition delay at low temperatures, and decreases it at high temperatures. Another important observation from the comparison of surrogate/H_2 versus surrogate/syngas blends in Figs. 5 and 6 is that the presence of CO decreases ignition delay for the blend at low temperatures, and has negligible effect at high temperatures. These results are consistent with those reported by Frassoldati et al. [69], and were further analyzed through sensitivity analysis in Sect. 3.5. An additional result for the ignition of *n*-$C_{12}H_{26}$/H_2/CO blends over a wider range of temperatures is shown in

[1] Further discussion on the NTC ignition behavior is provided in a later section.

[2] Ignition delay plots for wider temperature range including low temperatures are shown in Fig. 7.

Author's personal copy

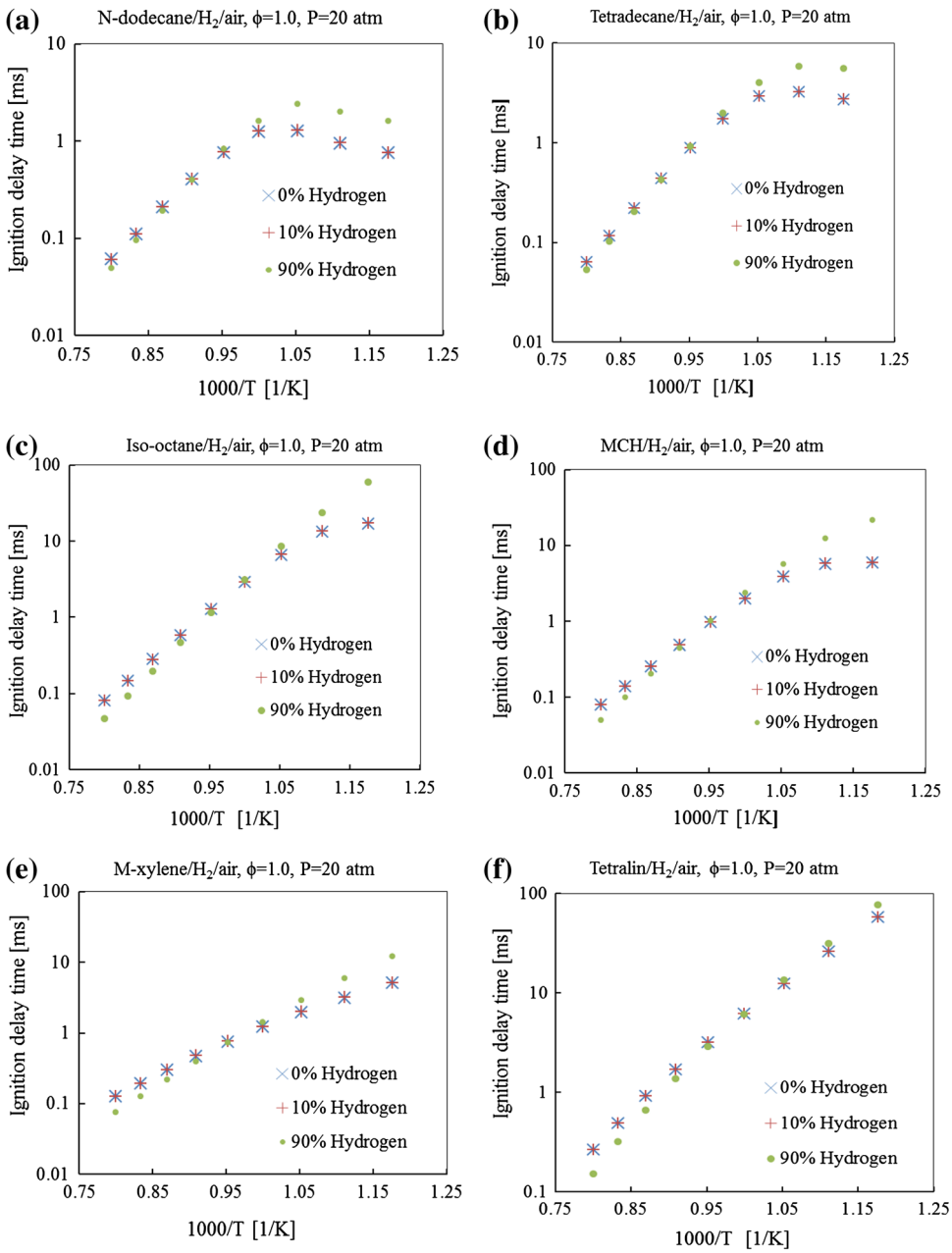

Fig. 2 Ignition delay plotted as a function of temperature for individual component/hydrogen blends with 0, 10, and 90 % H_2 by volume at P = 20 atm and $\phi = 1.0$

Fig. 7, which again indicates that H_2 or syngas addition in relatively large amounts increases the ignition delay of JP-8 surrogates at low temperatures, but decreases it at high temperatures.

Simulations were also performed to examine the effect of H_2 or syngas addition at different equivalence ratios. Figure 8 presents ignition delays for different Violi surrogate/H_2/CO blends containing 0 %, 10 % H_2, 90 % H_2, 10 % syngas, and 90 % syngas (50 % H_2/50 % CO), at $\phi = 0.7$ and 1.4. The ignition delay plots at these ϕ values are qualitatively similar to those at $\phi = 1.0$ shown in Fig. 6. Results concerning the effect of H_2 or syngas on the ignition of surrogate are also qualitatively similar for the three ϕ values. However, the ignition delays for the surrogate and blends decrease, and the NTC drop-off becomes sharper as ϕ is increased from 0.7 and 1.4, which is consistent with other studies.

3.4 Analysis of the negative temperature coefficient (NTC) region (*n*-dodecane)

The present study focuses on ignition at relatively high pressure and a range of temperatures relevant to many propulsion and energy conversion systems. For such conditions, the oxidation chemistry of large alkanes may be separated into three regions, namely low temperature

Author's personal copy

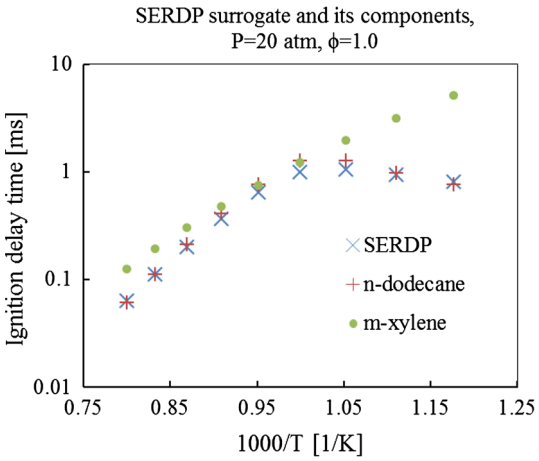

Fig. 3 Ignition delay plotted as a function of temperature for the SERDP surrogate and its two components at P = 20 atm and ϕ = 1.0

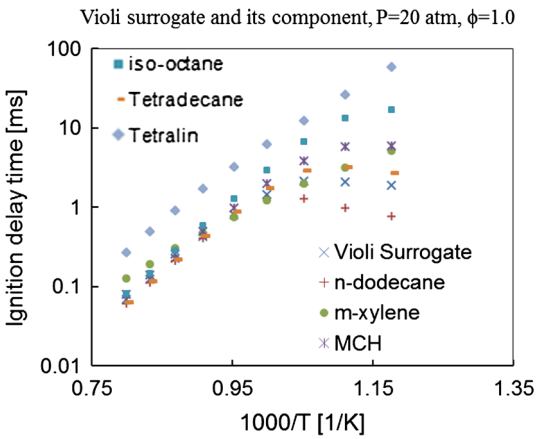

Fig. 4 Ignition delay plotted as a function of temperature for the Violi surrogate and its six components at P = 20 atm and ϕ = 1.0

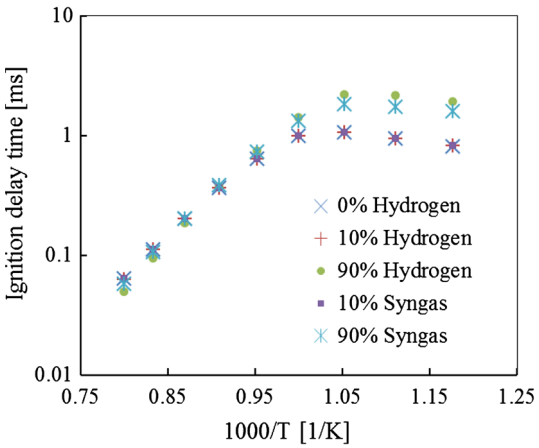

Fig. 5 Ignition delay plotted as a function of temperature for five SERDP/H_2/syngas blends at P = 20 atm and ϕ = 1.0

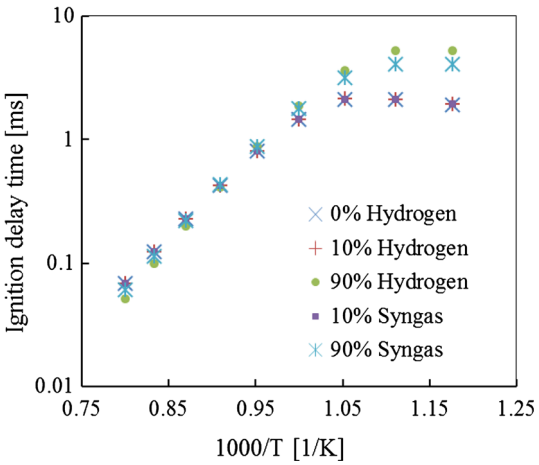

Fig. 6 Ignition delay plotted as a function of temperature for five Violi/H_2/syngas blends at P = 20 atm and ϕ = 1.0

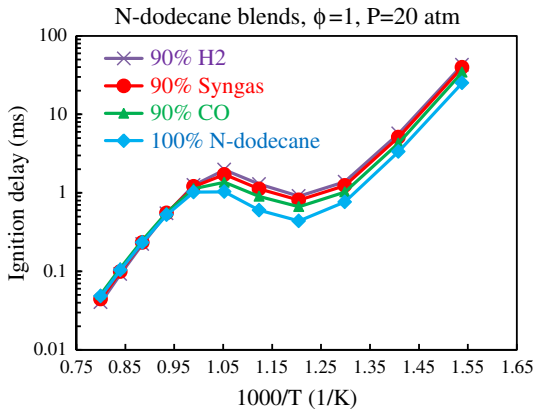

Fig. 7 Ignition delay plotted as a function of temperature for different blends of *n*-dodecane, H_2, CO, and syngas at P = 20 atm and ϕ = 1.0

region (650–800 K), intermediate temperature or NTC region (800–1,000 K), and high temperature region (above 1,000 K). Since these temperature regions are of critical importance for ignition in most combustion devices, a reaction path and sensitivity analysis was performed focusing on these regions. Results in the preceding sections indicated that as the temperature is increased, the ignition delays for both the surrogates decrease in the low and high temperature regions, but increase in the NTC region. Results also indicated that the ignition behavior of both SERDP and Violi surrogates is well represented by that of *n*-dodecane,[3] implying that the reaction path analysis can be performed using *n*-dodecane as the representative fuel. Important reactions identified from this analysis along with their kinetic parameters are listed in Table 2. Similar to the results reported in previous studies [70–72], the analysis

[3] Further confirmation is provided by the temporal evolution of key radical species such as HO2 presented in Figs. 14, 15, and 16.

Author's personal copy

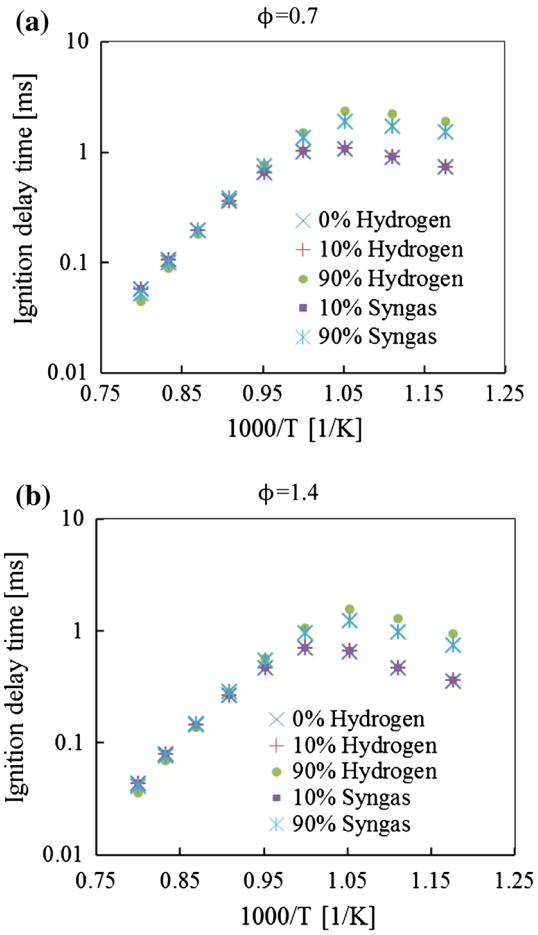

Fig. 8 Ignition delay plotted as a function of temperature for Violi/H_2/syngas blends at P = 20 atm and $\phi = 0.7$ (**a**) and $\phi = 1.4$ (**b**)

indicated that the ignition process is initiated by the production of alkyl radical ($NC_{12}H_{25}$) via reaction R1589.

$$O_2 + NC_{12}H_{26} \Rightarrow HO_2 + NC_{12}H_{25} \quad (R1589)$$

The ignition chemistry then follows two paths as determined by two competing reactions, R1665 and R1588, depending upon the temperature.

$$O_2 + NC_{12}H_{25} \Rightarrow NC_{12}H_{25}{-}OO \quad (R1665)$$

$$O_2 + NC_{12}H_{25} \Rightarrow 1.2NC_{10}H_{20} + HO_2 \quad (R1588)$$

Figure 9 plots the production/consumption rates of $NC_{12}H_{25}$ due to reactions R1588 and R1665 at T = 650 K. As inferred from this figure, the first path through R1665 dominates at low temperatures, producing alkylperoxy radicals ($N_{12}H_{25}$–OO) and leading to the following sequence of reactions:

$$NC_{12}H_{25}{-}OO \Rightarrow NC_{12}{-}QOOH \quad (R1667)$$

$$NC_{12}{-}QOOH + O_2 \Rightarrow NC_{12}{-}OOQOOH \quad (R1674)$$

$$NC_{12}{-}OOQOOH \Rightarrow NC_{12}{-}OQOOH + OH \quad (R1676)$$

$$NC_{12}{-}OQOOH \Rightarrow OH + .84C_2H_4CHO + .16CH_3COCH_2 + CH_3CHO + NC_7H_{14} \quad (R1679)$$

$$OH + NC_{12}H_{26} \Rightarrow H_2O + NC_{12}H_{25} \quad (R7312)$$

Thus the alkylperoxy radical isomerizes through R1667 to produce alkylhydroperoxy radical (QOOH), which reacts with O_2 to produce peroxyalkylhydroperoxy radical (OOQOOH) through R1674. Subsequently, peroxyalkylhydroperoxy decomposes through R1676 to produce ketohydroperoxide (OQOOH) and hydroxyl radical (OH). Further decomposition of ketohydroperoxide produces another hydroxyl radical (OH) through R1679. Consequently, there are sufficient OH radicals, which then react with the fuel through R7312 to produce more alkyl radicals to feed the R1665 chain. Thus a chain branching cycle is formed to produce more OH radicals to accelerate the ignition process. A reaction path diagram for this cycle, which is more dominant in the low temperature region, is shown in Fig. 10. Results of the sensitivity analysis are presented in Fig. 11, which plots the sensitivity coefficients with respect to important reactions at T = 650 K. These results provide further evidence of the dominant reactions associated with this path.

The second path initiated through R1588 is more dominant in the NTC region (800–1,000 K). At these temperatures, reactions R1588 and R1670 become important and generate hydroperoxy radical (HO_2) and alkene.

$$O_2 + NC_{12}H_{25} \Rightarrow 1.2NC_{10}H_{20} + HO_2 \quad (R1588)$$

$$NC_{12}{-}QOOH \Rightarrow 1.2NC_{10}H_{20} + HO_2 \quad (R1670)$$

$$HO_2 + HO_2 = H_2O_2 + O_2 \quad (R13)$$

Reaction R1670 involves the decomposition of alkylhydroperoxy radicals (QOOH), formed through R1667, by β-scission to produce alkene and HO_2. HO_2 radicals then lead to the formation of H_2O_2 through reaction R13. However, H_2O_2 is a metastable species at lower temperatures and thus slows down the ignition process in the NTC region. In addition, the reactivity of R1666 and R1675, which are the reverse reactions of R1665 and R1674, respectively, becomes high.

$$NC_{12}H_{25}{-}OO \Rightarrow NC_{12}H_{25} + O_2 \quad (R1666)$$

$$NC_{12}{-}OOQOOH \Rightarrow NC_{12}{-}QOOH + O_2 \quad (R1675)$$

These reactions revert to the formation of alkyl radical from alkylperoxy radical (R1666), and alkylhydroperoxy radical (QOOH) from peroxyalkylhydroperoxy radical (R1675). The alkyl and alkylhydroperoxy radicals then decompose through β-scission reactions to produce smaller alkyl radicals and alkene, as well as aldehyde and smaller alkanes. These reactions reduce the concentration of

Author's personal copy

Table 2 Important reactions for the ignition of *n*-dodecane/H_2 blends as assessed from sensitivity analysis

#	Reactions	A	b	E
1	$H + O_2 = OH + O$	2.21E+14	0.0	16,650
4	$H + O_2 + O_2 = HO_2 + O_2$	8.90E+14	0.0	−2,822
6	$H + HO_2 = OH + OH$	2.50E+14	0.0	1,900
13	$HO_2 + HO_2 = H_2O_2 + O_2$	2.11E+12	0.0	0.0
14	$OH + OH(+M) = H_2O_2(+M)$	7.40E+13	−0.4	0
19	$CO + OH = CO_2 + H$	9.60E+11	0.1	7,352.0
21	$CO + HO_2 = CO_2 + OH$	3.00E+13	0.0	23,000.0
257	$HO_2 + CH_3 = CH_3O + OH$	6.00E+12	0.0	0.0
372	$H + H_2O = H_2 + OH$	4.00E+10	1	19,000
1588	$O_2 + NC_{12}H_{25} \Longrightarrow 1.2NC_{10}H_{20} + HO_2$	5.00E+11	0.0	3,500
1589	$O_2 + NC_{12}H_{26} \Longrightarrow HO_2 + NC_{12}H_{25}$	3.00E+14	0.0	45,000
1665	$O_2 + NC_{12}H_{25} \Longrightarrow NC_{12}H_{25}$–OO	2.00E+12	0.0	0.0
1666	$NC_{12}H_{25}$–OO $\Longrightarrow NC_{12}H_{25} + O_2$	5.00E+13	0.0	31,000
1667	$NC_{12}H_{25}$–OO $\Longrightarrow NC_{12}$–QOOH	3.00E+12	0.0	24,000
1670	NC_{12}–QOOH $\Longrightarrow HO_2 + 1.2NC_{10}H_{20}$	4.50E+12	0.0	24,000
1674	NC_{12}–QOOH $+ O_2 \Longrightarrow NC_{12}$–OOQOOH	2.00E+12	0.0	0.0
1675	NC_{12}–OOQOOH $\Longrightarrow NC_{12}$–QOOH $+ O_2$	2.00E+14	0.0	29,000
1676	NC_{12}–OOQOOH $\Longrightarrow NC_{12}$–OQOOH $+$ OH	1.00E+12	0.0	23,000
7314	$HO_2 + NC_{12}H_{26} \Longrightarrow H_2O_2 + NC_{12}H_{25}$	1.18E+06	2	11,887.7

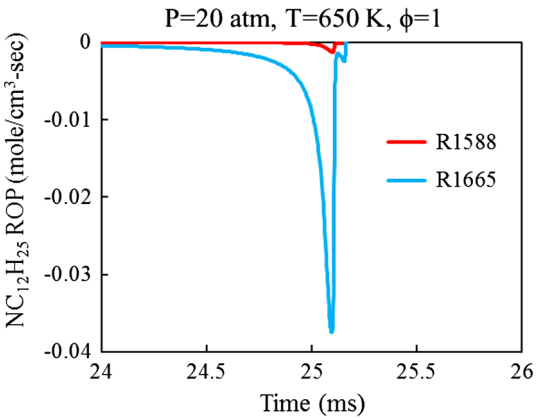

Fig. 9 Rate of production of $NC_{12}H_{25}$ due to reactions R1588 and R1665 at $\phi = 1.0$, P = 20 atm, and T = 650 K

alkylperoxy radicals, which are needed to drive the chain (R1665–R7312) discussed above, and also being endothermic, slow down the ignition process. Thus the net effect of R1588, R1670, R1666 and R1675 is mostly responsible for the NTC regime, where overall reactivity decreases because fewer radicals, especially OH, are produced.

As the temperature exceeds 1,000 K, the high temperature reactions become important. The reaction of HO_2 with the parent fuel produces hydrogen peroxide (H_2O_2) and alkyl radical through R7314. H_2O_2 then decomposes to form OH through the branching reaction R14, which provides the trigger for ignition in the high temperature region. The OH radicals thus react with fuel molecules to produce alkyl radicals and H_2O through R7312, which, with the large amount of heat release from this exothermal reaction, drives the high temperature ignition.

$$HO_2 + NC_{12}H_{26} \Rightarrow H_2O_2 + NC_{12}H_{25} \quad (R7314)$$

$$H_2O_2(+M) = OH + OH\ (+M) \quad (R14)$$

$$OH + NC_{12}H_{26} \Rightarrow H_2O + NC_{12}H_{25} \quad (R7312)$$

The role of important reactions, identified above, was further assessed by performing a sensitivity study in terms of ignition delay using the CRECK mechanism. The sensitivity coefficient S is defined as

$$S = \frac{\partial \ln \tau}{\partial \ln k} = \frac{k\partial\tau}{\tau\partial k} \quad (1)$$

Here k is the rate constant for a given reaction and τ is the ignition delay time. The value of S was obtained by changing the reaction rate constant by a factor of 2 and computing the corresponding ignition delay times. Then Eq. (1) yields

$$S = \frac{(\tau(2k) - \tau(k))}{\tau(k)} \quad (2)$$

Thus a negative S implies faster ignition as the given reaction rate is increased through k. Figure 12 presents the effect of temperature on the sensitivity coefficients of R1588, R1665, R1666, R1674, R1675, and R1670, for the ignition of *n*-$C_{12}H_{26}$/air mixtures at P = 20 atm and ϕ = 1. As anticipated, the sensitivity coefficients for R1665

Author's personal copy

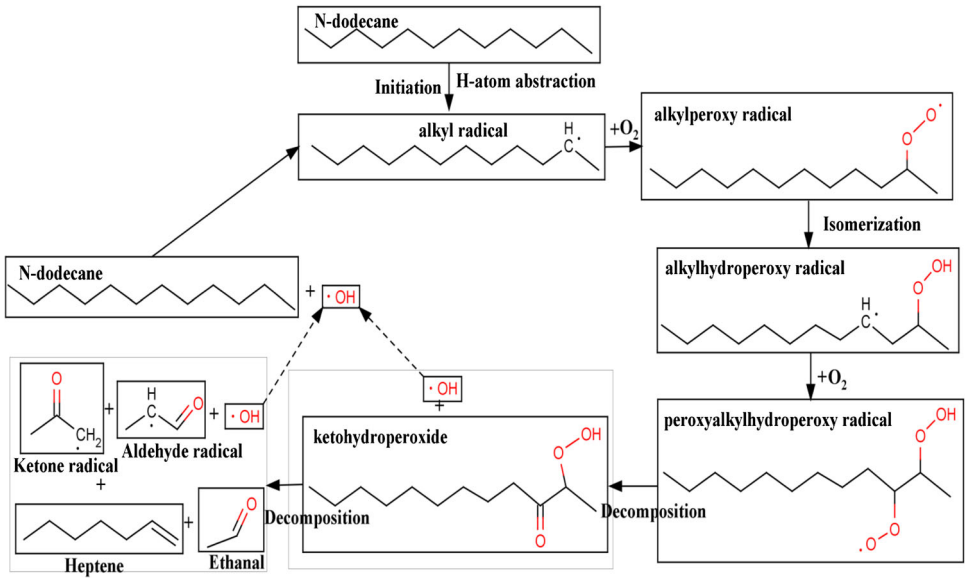

Fig. 10 Primary reaction path diagram describing *n*-dodecane oxidation at low temperatures

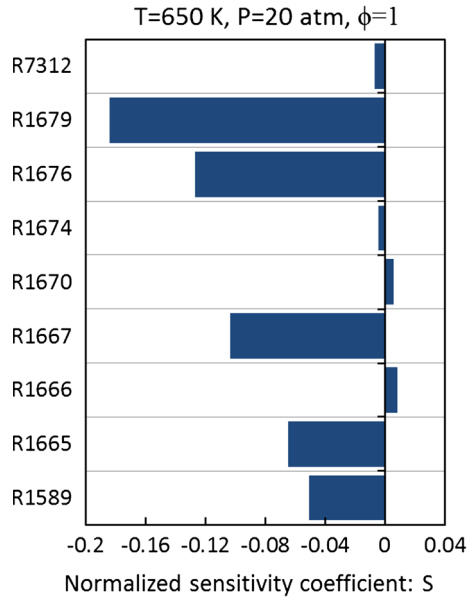

Fig. 11 Sensitivity coefficient for key reactions associated with the ignition of *n*-dodecane/air mixtures at 20 atm, T = 650 K and ϕ = 1.0

and R1674 have negative values, and thus decrease the ignition time, while those for R1588, R1670, R1666, and R1675 have positive values, and increase the ignition time. In addition, the sensitivity coefficients for R1588, R1670, R1666 and R1675 have their peak values in the NTC region (800–1,000 K). Also, the net effect of these four reactions far exceed the net effect of R14, R1665, and R1674 at the corresponding temperatures indicated in Fig. 13, implying that reactions R1588, R1666, R1675 and R1670 noticeably slow down ignition in the NTC region.

3.5 Sensitivity study on the effect of H_2 or syngas addition

Results in the preceding sections indicated that the addition of H_2 or syngas increases ignition delays for JP-8 surrogates in the NTC region. Since HO_2, OH, and H_2O_2 species play a major role in the ignition process, further insight on the effect of H_2 addition may be gained by examining the profiles of these species. Figure 14 presents the temporal variation of HO_2 mole fraction as the ignition process proceeds in time for the three *n*-$C_{12}H_{26}$/H_2 blends. For all three cases, the well-documented two-stage ignition is indicated, implying that even with 90 % H_2 in the blend, the ignition is predominantly determined by the hydrocarbon chemistry. The first HO_2 peak corresponding to the first-stage ignition is due to the production of this species through reactions R1589, R1588, and R1670 as discussed earlier. Subsequently, its mole fraction decreases as it gets converted to H_2O_2 via R13. This is further indicated in Fig. 15, which plots the temporal variation of HO_2, OH, and H_2O_2 for blends containing 0 and 90 % H_2. After the first-stage ignition, the ignition chemistry slows down due to the dominance of R1588 and R1670 in the NTC region, as noted earlier. Moreover, H_2O_2 being a metastable species at this temperature, it is slow to react. Consequently, its mole fraction slowly increases until the occurrence of second-stage ignition, which is indicated by a sharp drop in H_2O_2 mole fraction due to its conversion to OH radials. Also note that the first OH peak (cf. Fig. 15) is due to reactions R1676 and R1679, as discussed earlier, and its decrease after the first peak is due to R7312. Nevertheless, its concentration is much lower than that of HO_2, providing further evidence of slow ignition in the NTC region.

Author's personal copy

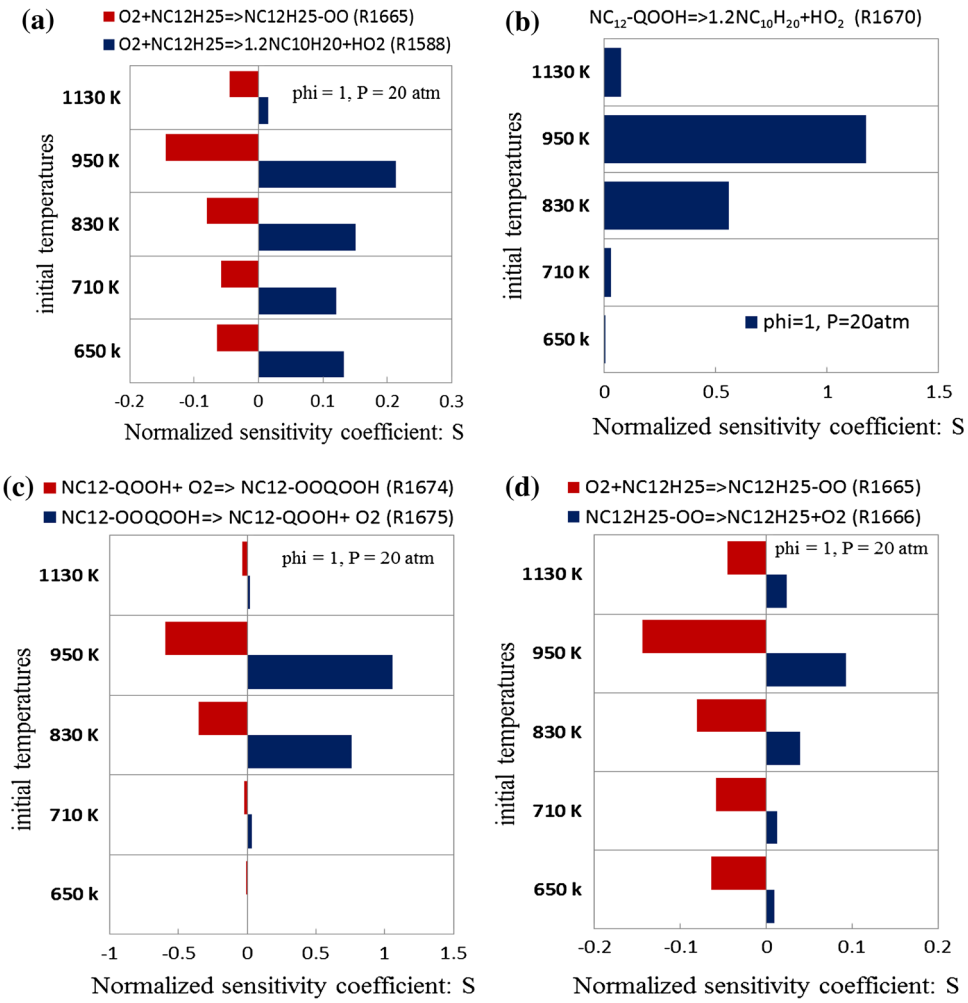

Fig. 12 Sensitivity coefficients for R1665 and R1588 (**a**), R1670 (**b**), R1674 and R1675 (**c**), and R1665 and R1666 (**d**), computed at different temperatures for *n*-dodecane/air mixtures at $\phi = 1.0$ and P = 20 atm

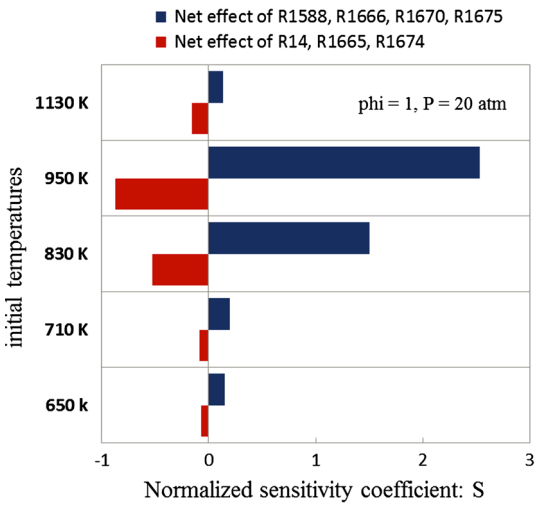

Fig. 13 Net values of sensitivity coefficients for R1588, R1666, R1670, and R1675 compared to that with respect to R14, R1665, and R1674; simulations performed at different initial temperatures for *n*-dodecane/air mixtures at $\phi = 1.0$ and P = 20 atm

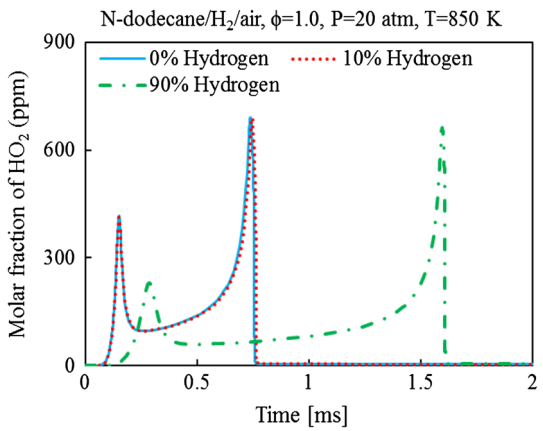

Fig. 14 Molar fraction of HO_2 versus time for the ignition of *n*-$C_{12}H_{26}/H_2$ blends with 0, 10, and 90 % H_2 at T = 850 K $\phi = 1.0$, P = 20 atm

The effect of H_2 or syngas on the ignition of JP-8 surrogates can be assessed using the temporal HO_2 profiles shown in Figs. 14 and 15. Similar plots for the ignition of SERDP/H_2/CO and Violi/H_2/CO blends are presented in

Author's personal copy

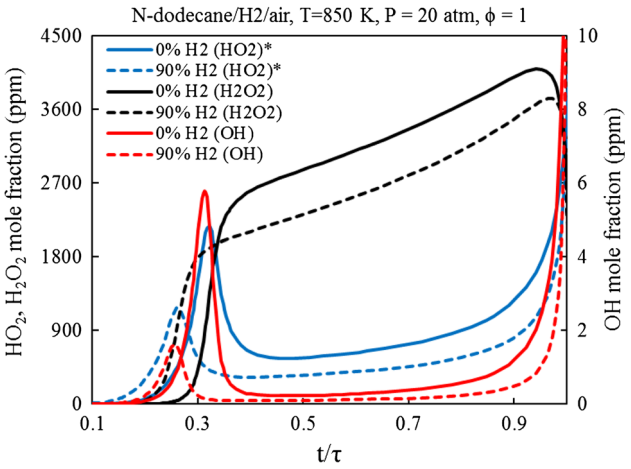

Fig. 15 Molar fractions of HO_2, H_2O_2 and OH versus t/τ for 0 % H_2 and 90 % H_2 in the *n*-dodecane/air blends at T = 850 K, P = 20 atm, ϕ = 1.0. The ignition delay τ = 0.4574 ms for 0 % H_2 and 1.0622 ms for 90 % H_2. *HO_2 is plotted to 5/1 *scale*

Fig. 16, which also shows the temporal evolution of temperature (Fig. 16a). The similarity between the HO_2 plots in Figs. 14 and 16 further confirm that *n*-dodecane may be used to represent the ignition characteristics of SERDP and Violi surrogates. These plots are consistent with the results discussed earlier that the addition of H_2 in small amount has no effect on the ignition of JP-8 surrogates, but in large amounts (80 % or higher), it causes a noticeable increase in ignition delay. Values of ignition delays for some representative cases are provided in Table 3. Furthermore, results indicate that the addition of 90 % H_2 or syngas to the blend decreases the peak mole fractions of HO_2, OH, and H_2O_2, as well as the peak temperature corresponding to the first-stage ignition. It addition, it noticeably increases both the first and the second ignition delays, and thus the total ignition delay. The increase in the first ignition delay may be attributed to two factors. One is due to a reduction in the amount of hydrocarbon fuel in the blend, which slows down the low temperature reaction path discussed earlier, and also decreases the concentrations HO_2, H_2O_2, and OH. Another factor is the consumption of OH radicals due to the presence of H_2 or syngas in the blend. This aspect is further discussed below through a sensitivity analysis that identifies the important reactions for the ignition of *n*-$C_{12}H_{26}$/H_2/CO blends. The second-stage ignition delay is also considerably increased for the 90 % H_2 and 90 % syngas cases, since the peak temperature and peak concentrations of radical species at the time of first ignition are lower. Another factor is the consumption of

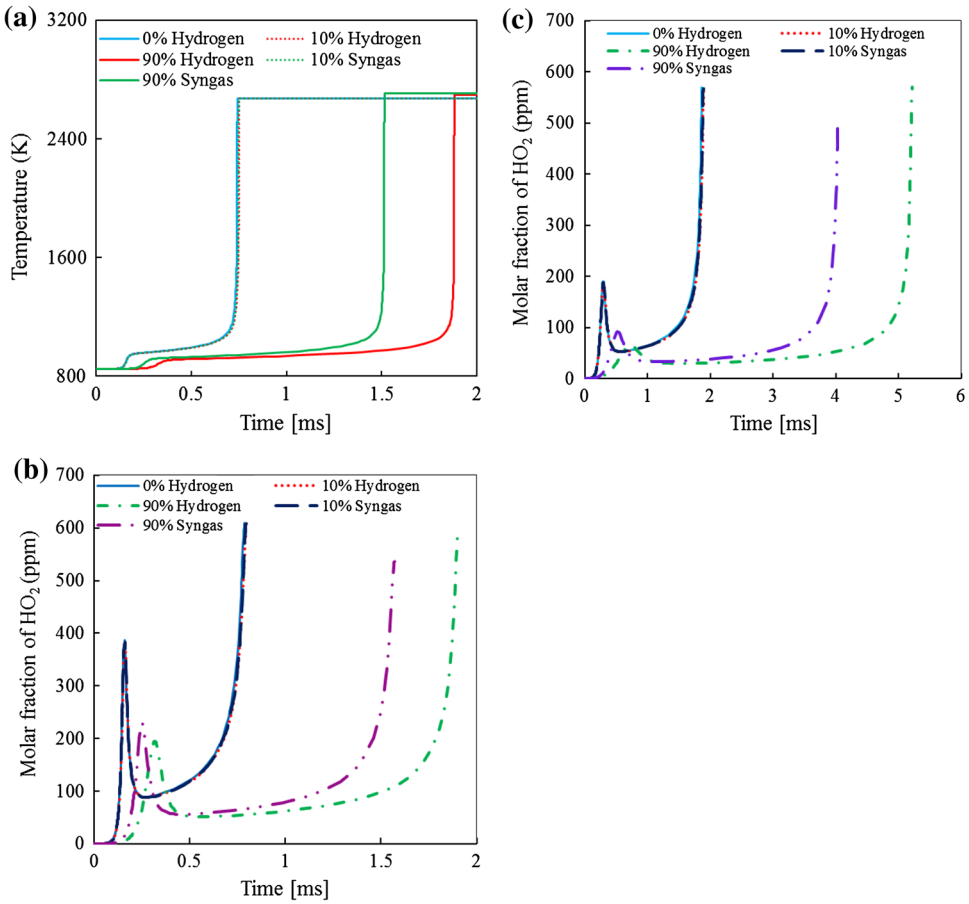

Fig. 16 Temperatures versus time for SERDP/H_2/syngas blends (**a**), mole fraction of HO_2 versus time for SERDP/H_2/syngas blends (**b**) and Violi/H_2/Syngas/blends (**c**) at T = 850 K, ϕ = 1.0, and P = 20 atm

Author's personal copy

Table 3 Ignition delay values for some representative cases showing the effect of H_2 and syngas on the ignition of JP-8 surrogate

Ignition delay (ms)	T = 830 K	T = 1,250 K
0 % H_2	0.4380	0.0482
80 % H_2	0.6355	0.0438
90 % H_2	1.0622	0.0402
98 % H_2	13.9192	0.0223
90 % Syngas	0.8641	0.0444

P = 20 atm, ϕ = 1

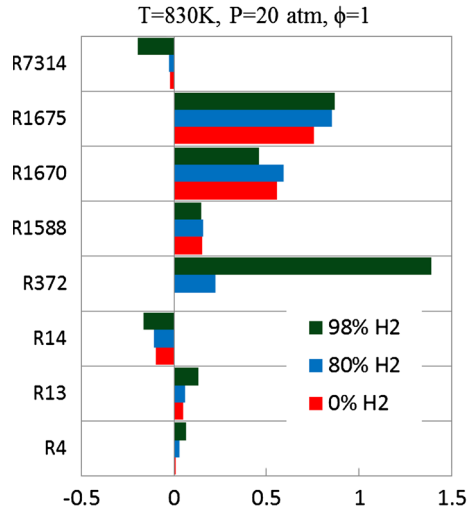

Fig. 17 Sensitivity coefficients for the ignition of *n*-dodecane/H_2 blends at 830 K, ϕ = 1.0, and P = 20 atm. Blends contain 0 % H_2, 80 % H_2, and 98 % H_2

OH radicals due to the presence of H_2 or syngas in the blend as stated above.

Figure 17 presents the computed sensitivity coefficients of the important reactions for the ignition of *n*-dodecane/H_2 blends in the NTC region. For the 0 % H_2 case, the results are consistent with those discussed earlier, i.e., the hydrocarbon chemistry in the NTC region is dominated by reactions R1588, R1670, and R1675. For the 80 % H_2 and 98 % H_2 cases, results indicate that the sensitivity to above reactions remain essentially unaltered with H_2 addition. More importantly, Fig. 17 indicates that reaction R372 ($H_2 + OH = H_2O + H$) plays an increasingly significant role and slows down ignition in the NTC region as the amount of H_2 in the blend is increased. Note that for the present conditions, i.e., low temperature and high H_2 concentration, this reaction is endothermic and consumes hydroxyl radicals. Thus the increased ignition delays caused by H_2 addition in the NTC region can mainly be attributed to R372.

In order to characterize the effect of H_2 at high temperatures, Fig. 18 presents the sensitivity coefficients for

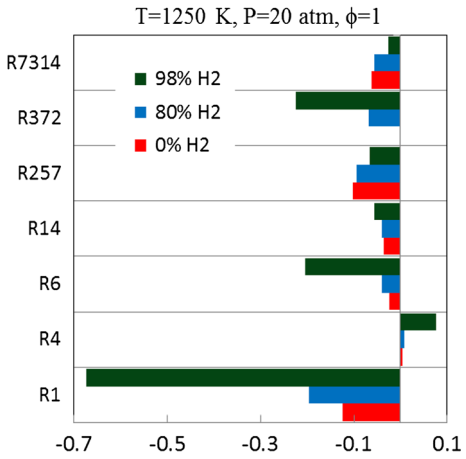

Fig. 18 Sensitivity coefficients for the ignition of *n*-dodecane/H_2 blends at T = 1250 K, ϕ = 1.0, and P = 20 atm. Blends contain 0 % H_2, 80 % H_2, and 98 % H_2

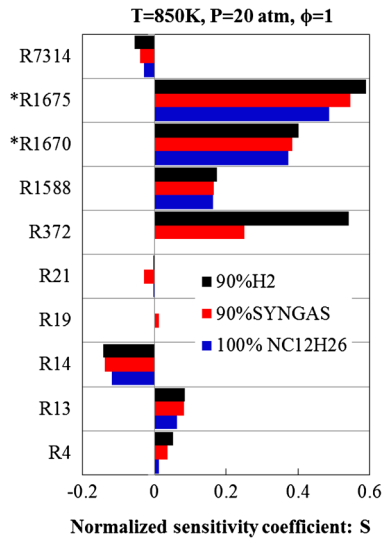

Fig. 19 Sensitivity coefficients for the ignition of *n*-dodecane/H_2/CO blends at T = 850 K, ϕ = 1.0, and P = 20 atm. Blends contain 0 % H_2, 90 % H_2, and 90 % syngas. *Plotted to 1/2 *scale*

the ignition of *n*-dodecane/H_2 blends at T = 1,250 K. As discussed earlier, the addition of H_2 in large amounts at these temperatures decreases the ignition delay of blends. Results in Fig. 18 indicate that this is mainly due to reactions R1 ($H + O_2 = OH + O$), R6 ($H + HO_2 = O-H + OH$) and R372. Since these reactions represent important steps in H_2 oxidation, the implication is that with more than 80 % H_2 addition, the ignition chemistry of blends is increasingly being dominated by H_2 oxidation chemistry. Thus as the amount of H_2 in the blend is increased, these three reactions become significant and enhance the ignitability. Note that the sensitivity of R372 reverses sign from NTC region to high temperature region. As the amount of H_2 in the blend is increased, the reactivity

Author's personal copy

of R372 increases. This produces more H radicals, which then react with O2 (reaction R1) and HO2 (reaction R6) to produce more OH radicals, with the net effect that the ignition process is noticeably accelerated in the high temperature region.

A sensitivity study was also performed to characterize the effect of syngas, or the presence of CO, on the ignition of JP-8 surrogates. As noted earlier, increasing the amount of CO in syngas leads to a decrease in ignition delay at low temperatures including the NTC region, but has negligible effect at high temperatures. Figure 19 presents the results of sensitivity analysis for the ignition of blends containing 0 % H_2, 90 % H_2, and 90 % syngas at 850 K. The effect of H_2 addition on the sensitivity coefficients has already been discussed in the context of Fig. 17. The comparison of 90 % H_2, and 90 % syngas cases indicates that the hydrocarbon chemistry is not much affected by the presence of CO. The main effect of CO appears to be a reduction in the relative importance of reaction R372, which was demonstrated to be the primary cause for increasing the ignition delays with H_2 addition. Thus the presence of CO in syngas primarily reduces the effectiveness of H_2 in increasing the ignition delay of JP-8 surrogate in the NTC region. It should also be noted that reaction R19 ($CO + OH = CO_2 + H$) does not play a significant role in the ignition of JP-8/syngas blends in the NTC region.

4 Conclusions

A computational study has been performed to examine the effect of hydrogen and syngas addition on the ignition of two JP-8 fuel surrogates, namely a two-component (SERDP) and a six-component (Violi) surrogate. The Violi surrogate has previously been found to accurately simulate the smoke point, volatility, flame temperature profiles, and extinction limits of JP-8, while the SERDP surrogate has been shown to reproduce the flame structure predicted with the Violi surrogate. The computational model is used on the CHEMKIN software along with a detailed CRECK-0810 reaction mechanism, containing 341 species and 9,173 reactions, and has been validated for the ignition of hydrogen/air, syngas/air, and *n*-dodecane/air mixtures at engine relevant conditions. The ignition behavior of JP-8 surrogate/H_2/CO mixtures has been examined at temperatures between 650 and 1,250 K, pressure = 20 atm, and $\phi = 0.7$, 1.0 and 1.4. The sensitivity analysis is performed to provide further insight into the effects of H_2 and syngas on the ignition of JP-8 surrogates. Important observations follow.

For the conditions investigated, the ignition characteristics of JP-8 surrogates, including the two-stage ignition and NTC behavior, can be well represented by *n*-dodecane. The addition of H_2 or syngas in relatively small quantities has no effect on the ignition of surrogates or any of their components. However, H_2 or syngas addition in larger amounts (more than 80 % by volume) increases the ignition delay for JP-8 surrogates/air mixtures at low temperatures, and decreases it at high temperatures. Increasing the amount of CO in syngas decreases the ignition delay of surrogate/syngas blends in the low temperature and NTC regions, but has negligible effect at high temperatures.

The reaction path analysis indicates that the ignition of JP-8 surrogates at low temperatures is characterized by two competing paths. The first path, which is favored at low temperatures ($T < 800$), involves the production of keto-hydroperoxide radicals, which decompose and increase the system reactivity leading to the first-stage ignition. The second path becomes dominant in the NTC region ($800 < T < 1000$ K), and involves the decomposition of alkyl and alkylhydroperoxy radicals, leading to a drop in overall reactivity.

The sensitivity analysis further indicates that in the low temperature and NTC regions, the addition of H_2 depletes the OH radical pool mainly through reaction R372: $H_2 + OH = H_2O + H$. This increases the first-stage ignition delay and reduces the temperature rise associated with the first-stage ignition process. As a consequence, the second-stage ignition and the total ignition delays increase. On the other hand, H_2 addition at high temperatures ($T >$ 1000 K) reduces ignition delay due to reactions: $H_2O_2 + M = 2OH + M$, $H_2 + OH = H_2O + H$, $H + O_2 = OH + O$, and $H + HO_2 = OH + OH$, which produce ample hydroxyl radicals and expedite ignition. Increasing the amount of CO in syngas reduces the effectiveness of R372, and thus reduces the ignition delay of JP-8/syngas blends in the low temperature and NTC regions. The reaction: $CO + OH = CO_2 + H$ does not play a significant role in the ignition of JP-8/syngas blends in this temperature regime.

These results may be of interest for the development of diesel and gas turbine engines using JP-8/H_2 or JP-8/syngas blends. The results may also be relevant for gasoline and diesel fuels, which typically contain straight-chain, branched-chain, and cyclo-paraffins, and aromatics.

References

1. Aggarwal, S.K.: Simulations of combustion and emissions characteristics of biomass-derived fuels. In: Dahlquist, E. (ed.) Technologies for Converting Biomass to Useful Energy: Combustion, Gasification, Pyrolysis, Torrefaction and Fermentation. CRC Press, Boca Raton (2013)
2. Elliot, F.G., Kurz, R., Ethridge, C., O'Connell, J.P.: Fuel suitability considerations for industrial gas turbines. J. Eng. Gas Turbines Power **126**, 119–126 (2004)
3. Maschio, G., Lucchesi, A., Stoppato, G.: Production of syngas from biomass. Bioresour. Technol. **48**, 119–126 (1994)

Author's personal copy

4. Goransson, K., Soderlind, U., He, J., Zhang, W.: Review of syngas production via biomass DFBGs. Renew. Sustain. Energy Rev. **15**, 482–492 (2011)
5. Hansen, A.C., Zhang, Q., Lyne, P.W.L.: Ethanol-diesel fuel blends—a review. Bioresour. Technol. **96**, 277–285 (2005)
6. Cho, H.M., He, B.-Q.: Spark ignition natural gas engines—a review. Energy Convers. Manage. **48**(2), 608–618 (2007)
7. Morrone, B., Andrea, U.: Numerical investigation on the effects of natural gas and hydrogen blends on engine combustion. Int. J. Hydrogen Energy **34**, 4626–4634 (2009)
8. Aggarwal, S.K.: Hydrogen-assisted combustion and emission characteristics of fossil fuels. In: Lackner, M., Winter, F., Agarwal, A.K. (eds.) Handbook of Combustion, vol. 3. Wiley, New York (2010). ISBN 978-3-527-32449-1
9. Guo, H., Smallwood, G.J., Liu, F., Ju, Y., Gulder, O.L.: The effect of hydrogen addition on flammability limit and NO_x emission in ultra-lean counterflow CH_4/air premixed flames. Proc. Combust. Inst. **30**, 303–311 (2005)
10. Yu, G., Law, C.K., Wu, C.K.: Laminar flame speeds of hydrocarbon + air mixtures with hydrogen addition. Combust. Flame **63**, 339–347 (1986)
11. Halter, F., Chauveau, C., Djebaili-Chaumeix, N., Gokalp, I.: Characterization of the effects of pressure and hydrogen concentration on laminar burning velocities of methane-hydrogen-air mixtures. Proc. Combust. Inst. **30**, 201–208 (2005)
12. Shy, S.S., Chen, Y.C., Yang, C.H., Liu, C.C., Huang, C.M.: Effects of H_2 or CO_2 addition, equivalence ratio, and turbulent straining on turbulent burning velocities for lean premixed methane combustion. Combust. Flame **153**, 510–524 (2008)
13. Tuncer, O., Acharya, S., Uhm, J.H.: Dynamics, NO_x and flashback characteristics of confined premixed hydrogen-enriched methane flames. Int. J. Hydrogen Energy **34**, 496–506 (2009)
14. Briones, A.M., Aggarwal, S.K., Katta, V.R.: Effects of H_2 enrichment on the propagation characteristics of CH_4-air triple flames. Combust. Flame **153**, 367–383 (2008)
15. Naha, S., Aggarwal, S.K.: Fuel effects on NO_x emissions in partially premixed flames. Combust. Flame **39**, 90–105 (2004)
16. Naha, S., Briones, A.M., Aggarwal, S.K.: Effect of fuel blends on pollutants emissions in flames. Combust. Sci. Technol. **177**(1), 183–220 (2005)
17. Guo, H., Neill, W.S.: A numerical study on the effect of hydrogen/reformate gas addition on flame temperature and NO formation in strained methane/air diffusion flames. Combust. Flame **156**, 477–483 (2009)
18. Schefer, R.W., Wicksall, D.M., Agrawal, A.K.: Combustion of hydrogen-enriched methane in a lean premixed swirl-stabilized burner. Proc. Combust. Inst. **29**, 843–851 (2002)
19. Schefer, R.W.: Hydrogen enrichment for improved lean flame stability. Int. J. Hydrogen Energy **28**, 1131–1141 (2003)
20. Safta, C., Madnia, C.K.: Autoignition and structure of nonpremixed CH_4/H_2 flames: detailed and reduced kinetic models. Combust. Flame **144**, 64–73 (2006)
21. Halter, F., Chauveau, C., Gokalp, I.: Characterization of the effects of hydrogen addition in premixed methane/air flames. Int. J. Hydrogen Energy **32**, 2585–2592 (2007)
22. Choudhuri, A.R., Gollahalli, S.R.: Characteristics of hydrogen–hydrocarbon composite fuel turbulent jet flames. Int. J. Hydrogen Energy **28**, 445–454 (2003)
23. Kim, H.S., Arghode, V.K., Linck, M.B., Gupta, A.K.: Hydrogen addition effects in a confined swirl-stabilized methane-air flame. Int. J. Hydrogen Energy **34**, 1045–1053 (2009)
24. Gersen, S., Anikin, N.B., Mokhova, A.V., Levinsky, H.B.: Ignition properties of methane/hydrogen mixtures in a rapid compression machine. Int. J. Hydrogen Energy **33**, 1957–1964 (2008)
25. Huang, J., Bushe, W.K., Hill, P.G., Munshi, S.R.: Shock initiated ignition in homogeneous methane-hydrogen-air mixtures at high pressure. Int. J. Chem. Kinet. **38**(4), 221–233 (2006)
26. Fotache, C.G., Kreutz, T.G., Law, C.K.: Ignition of hydrogen-enriched methane by heated air. Combust. Flame **110**, 429–440 (1997)
27. Bauer, C.G., Forest, T.W.: Effect of hydrogen addition on the performance of methane-fueled vehicles. Part I: effect on SI engine performance. Int. J. Hydrogen Energy **26**, 55–70 (2001)
28. Bauer, C.G., Forest, T.W.: Effect of hydrogen addition on performance of methane-fueled vehicles. Part II: driving cycle simulation. Int. J. Hydrogen Energy **26**, 71–90 (2001)
29. Liu, Z., Karim, G.A.: Knock characteristics of dual-fuel engines fueled with hydrogen fuel. Int. J. Hydrogen Energy **20**, 919–924 (1995)
30. Nagalingam, B., Duebel, F., Schmillen, K.: Performance study using natural gas, hydrogen supplemented natural gas and hydrogen in AVL research engine. Int. J. Hydrogen Energy **8**(9), 715–720 (1983)
31. Ma, F., Wang, Y., Liu, H., Li, Y., Wang, J., Zhao, S.: Experimental study on thermal efficiency and emission characteristics of a lean burn hydrogen enriched natural gas engine. Int. J. Hydrogen Energy **32**, 5067–5075 (2007)
32. Wang, J., Chen, H., Liu, B., Huang, Z.: Study of cycle-by-cycle variations of a spark ignition engine fueled with natural gas-hydrogen blends. Int. J. Hydrogen Energy **33**, 4876–4883 (2008)
33. Das, L.M., Gulati, R., Gupta, P.K.: A comparative evaluation of the performance characteristics of a spark ignition engine using hydrogen and compressed natural gas as alternative fuels. Int. J. Hydrogen Energy **25**, 783–793 (2000)
34. Kahraman, N., Ceper, B., Akansu, S.O., Aydin, K.: Investigation of combustion characteristics and emissions in a spark-ignition engine fuelled with natural gas-hydrogen blends. Int. J. Hydrogen Energy **34**(2), 1026–1034 (2009)
35. Dimopoulos, P., Bach, C., Soltic, P., Boulouchos, K.: Hydrogen-natural gas blends fuelling passenger car engines: combustion, emissions and well-to-wheels assessment. Int. J. Hydrogen Energy **33**, 7224–7236 (2008)
36. Sher, E., Hacohen, Y.: Measurements and predictions of the fuel consumption and emission of a spark ignition engine fueled with hydrogen-enriched gasoline. J Power Energy **203**, 155–159 (1989)
37. Changwei, J., Shuofeng, W.: Effect of hydrogen addition on the idle performance of a spark ignited gasoline engine at stoichiometric condition. Int. J. Hydrogen Energy **34**, 3546–3556 (2009)
38. Shirk, M.G., McGuire, T.P., Neal, G.L., Haworth, D.C.: Investigation of a hydrogen-assisted combustion system for a light-duty diesel vehicle. Int. J. Hydrogen Energy **33**, 7237–7244 (2008)
39. Sahoo, B.B., Sahoo, N., Saha, U.K.: Effect of H2:CO ratio in syngas on the performance of a dual fuel diesel engine operation. Appl. Therm. Eng. **49**, 139–146 (2012)
40. Shudo, T., Yamada, H.: Hydrogen as an ignition-controlling agent for HCCI combustion engine by suppressing the low-temperature oxidation. Int. J. Hydrogen Energy **32**, 3066–3072 (2007)
41. Subramanian, G., Da Cruz, A.P., Bounaceur, R., Vervisch, L.: Chemical impact of CO and H_2 addition on the auto-ignition delay of homogeneous *n*-heptane/air mixtures. Combust. Sci. Technol. **179**, 1937–1962 (2007)
42. Thiessen, S., Khalil, E., Karim, G.: The autoignition in air of some binary fuel mixtures containing hydrogen. Int. J. Hydrogen Energy **35**, 10013–10017 (2010)
43. Aggarwal, S.K., Awomolo, O., Akber, K.: Ignition characteristics of heptane-hydrogen and heptane-methane fuel blends at elevated pressures. Int. J. Hydrogen Energy **36**, 15392–15402 (2011)

Author's personal copy

44. Jain, S., Li, D., Aggarwal, S.K.: Effect of hydrogen and syngas addition on the ignition of *iso*-octane/air mixtures. Int. J. Hydrogen Energy **38**, 4163–4176 (2013)
45. Edwards, T., Maurice, L.Q.: Surrogate mixtures to represent complex aviation and rocket fuel. J. Propuls. Power **17**(2), 461–466 (2001)
46. Heneghan, S.P., Locklear, S.L., Geiger, D.L., Anderson, S.D., Schulz, W.D.: Static tests of jet thermal and oxidative stability. J. Propuls. Power **9**(1), 5–9 (1993)
47. Katta, V.R., Meyer, T.R., Montgomery, C.J., Roquemore, W.M.: Studies on soot formation in a model gas-turbine combustor. In: 41st AIAA/ASME/SAE/ASEE Joint Propulsion Conference Exhibit, Paper No. AIAA 2005-3777 (2005)
48. Far, E.K., Parsinejad, F., Metghalchi, H.: Flame structure and laminar burning speeds of JP-8/air premixed mixtures at high temperatures and pressures. Fuel **89**, 1041–1049 (2010)
49. Humer, S., Frassoldati, A., Granata, S., Faravelli, T., Ranzi, E., Seiser, R., Seshadri, K.: Experimental and kinetic modeling study of combustion of JP-8, its surrogates and reference components in laminar nonpremixed flows. Proc. Combust. Inst. **31**, 393–400 (2007)
50. Cooke, J.A., Bellucci, M., Smooke, M.D., Gomex, A., Violi, A., Faravelli, T., Ranzi, E.: Computational and experimental study of JP-8, a surrogate, and its components in counterflow diffusion flames. Proc. Combust. Inst. **30**, 439–446 (2005)
51. Far, E.K., Moghaddas, A., Metghalchi, H., Keck, J.C.: The effect of diluent on flame structure and laminar burning speeds of JP-8/oxidizer/diluent premixed flames. Fuel **90**, 1476–1486 (2011)
52. Holley, A.T., Dong, Y., Andac, M.G., Egolgopoulos, F.N., Edwards, T.: Ignition and extinction of non-premixed flames of single-component liquid hydrocarbons, jet fuels, and their surrogates. Proc. Combust. Inst. **31**, 1205–1213 (2007)
53. Mensch, A., Santoro, R.J., Litzinger, T.A., Lee, S.Y.: Sooting characteristics of surrogates for jet fuels. Combust. Flame **157**, 1097–1105 (2010)
54. Henriksen, T.L., Nathan, G.J., Alwahabi, Z.T., Qamar, N., Ring, T.A., Eddings, E.G.: Planar measurements of soot volume fraction and OH in a JP-8 pool fire. Combust. Flame **156**, 1480–1492 (2009)
55. Topal, M.H., Wang, J., Levendis, Y.A., Carlson, J.B., Jordan, J.: PAH and other emissions from burning of JP-8 and diesel fuels in diffusion flames. Fuel **83**, 2357–2368 (2004)
56. Sochet, I., Gillard, P.: Flammability of kerosene in civil and military aviation. J. Loss Prev. Process Ind. **15**, 335–345 (2002)
57. Vasu, S.S., Davidson, D.F., Hanson, R.K.: Jet fuel ignition delay times: Shock tube experiments over wide conditions and surrogate model predictions. Combust. Flame **152**, 125–143 (2008)
58. Kumar, K., Sung, C.J.: An experimental study of the autoignition characteristics of conventional jet fuel/oxidizer mixtures: Jet-A and JP-8. Combust. Flame **157**, 676–685 (2010)
59. Katta, V.R., Roquemore, W.M.: Calculation of JP-8 jet diffusion flames using a semi-detailed chemical mechanism. In: 2010 Spring Technical Meeting, Central States Section of the Combustion Institute, Champaign, IL, March 21–23, 2010
60. Violi, A., Yan, S., Eddings, E.G., Sarofim, A.F., Granata, S., Faravelli, T., Ranzi, E.: Experimental formulation and kinetic model for JP-8 surrogate mixtures. Combust. Sci. Technol. **174**(11–12), 399–417 (2002)
61. Katta, V.R., Roquemore, W.M.: Performance of JP-8 surrogates and parent species in a swirl combustor. ASME Paper GT2010-22301. In: Proceedings ASME Turbo Expo, Glasgow, UK, June 14–18, 2010
62. Kee, R.J., Rupley, F.M., Miller, J.A.: CHEMKIN Collection, Release 3.6. Reaction Design Inc, San Diego (2000)
63. Ranzi, E.: http://creckmodeling.chem.polimi.it/kinetic.htm. Accessed Oct 2012
64. Grana, R., Seshadri, K., Cuoci, A., Niemann, U., Faravelli, T., Ranzi, E.: Kinetic modelling of extinction and autoignition of condensed hydrocarbon fuels in non-premixed flows with comparison to experiment. Combust. Flame **159**(1), 130–141 (2012)
65. O'Connaire, M., Curran, H.J., Simmie, J.M., Pitz, W.J., Westbrook, C.K.: A comprehensive modeling study of hydrogen oxidation. Int. J. Chem. Kinet. **36**, 603–622 (2004)
66. Davis, S.G., Joshi, A.V., Wang, H., Egolfopoulos, F.: An optimized kinetic model of H_2/CO combustion. Proc. Combust. Inst. **30**, 1283–1292 (2005)
67. Petersen, E.L., Kalitan, D.M., Barrett, A.B., Reehal, S.C., Mertens, J.D., Beerer, D.J., Hack, R.L., McDonell, V.G.: New syngas/air ignition data at lower temperature and elevated pressure and comparison to current kinetic models. Combust. Flame **149**, 244–247 (2007)
68. Dryer, F.L., Chaos, M.: Ignition of syngas/air and hydrogen/air mixtures at low temperatures and high pressures: experimental data interpretation and kinetic modeling implications. Combust. Flame **152**, 293–299 (2008)
69. Frassoldati, A., Faravelli, T., Ranzi, E.: The ignition, combustion and flame structure of carbon monoxide/hydrogen mixtures. Note 1: detailed kinetic modeling of syngas combustion also in presence of nitrogen compounds. Int. J. Hydrogen Energy **32**, 3471–3485 (2007)
70. Curran, H.J., Gaffuri, P., Pitz, W.J., Westbrook, C.K.: A comprehensive modeling Study of *iso*-octane oxidation. Combust. Flame **129**, 253–280 (2002)
71. Curran, H.J., Pitz, W.J., Westbrook, C.K., Callahan, C.V., Dryer, F.L.: Oxidation of automotive primary reference fuels at elevated pressures. Proc. Combust. Inst. **27**, 379–387 (1998)
72. Natelson, R.H.: Preignition and autoignition behavior of the xylene isomers. http://hdl.handle.net/1860/3192. Accessed Oct 2012